Numerical analysis on the effect of the intermediate diaphragm on the concrete bridge to the acceleration and frequency under moving load

Ir. Wan Ikram Wajdee Wan Ahmad Kamal[1], Izni Syahrizal Ibrahim[2], Khairul Hazman Padil[2], Sarehati Umar[1], Han-Seung Lee[3] and Jitendra Kumar Singh[3]

[1]School of Civil Engineering, Faculty of Engineering, Universiti Teknologi Malaysia, 81310 Johor Bahru, Johor, Malaysia
[2] Forensic Engineering, Centre, Institute of Smart Infrastructure and Innovative Construction, School of Civil Engineering, Faculty of Engineering, Universiti Teknologi Malaysia, 81310 Johor Bahru, Johor, Malaysia
[3] Innovative Durable Building and Infrastructure Research Center, Hanyang University, Ansan, South Korea

Corresponding author's e-mail: wanikramwajdee@utm.my

Abstract. For the goal of construction simplicity, when considering the addition of an intermediate diaphragm (ID) to the bridge deck construction, particularly for beam-to-slab bridges, the majority of engineers were found to be passive. This took place as a result of the perception that ID does not significantly contribute to improving structural capacity, particularly for bridge deck structures and structurally as a whole. The constructability issue now is also playing an issue for this beam-to-slab bridge, which has been thought to slow down the construction speed since its location in the middle of the span is an unsupported region, which makes it a bit difficult to fix and cast both reinforcement and concrete. As a result of the omittance of ID, adverse impacts have taken place on the beam slab bridge, particularly on the medium span where moderate vibration has been triggered, which is categorized as minor resonance due to traffic crossing, primarily big trucks being loaded, on the bridge deck itself. The results of the numerical study using Abaqus software, it was revealed that the presence of ID improved the vibration level in terms of acceleration and natural frequency, resulting in significant improvements in riding comfort.

1. Introduction

An intermediate diaphragm (ID) in a bridge is a structural member designed as a secondary member to brace the main girders from excessive deflection and rotation due to the eccentric load of the vehicle wheels. In addition, ID had also been applied to stiffen the bridge deck structure in resisting collision impact from traffic load of either heavy trucks or passenger cars [1], [2]. There are cases where ID had extensively been used in beam-to-slab bridges to facilitate the distribution of bending moment and shear force from the live load. AASHTO had stipulated the usage of ID in bridge design [3]–[5]. Usually, this ID member is arranged within the span of the bridge. Presently, there are no regulations in terms of spacing, sizing and number of IDs in the bridge span provided by the Code of Practice [6]. Thus, any practising or implementation on the application of ID against the bridge deck in terms of spacing and sizing is based on the designer's judgment through the structural detail analysis. There are cases where

the partial depth of ID was applied to the bridge deck for the sake of the load distribution mechanism [7], [8]. In the past event, the end diaphragm had been affected by seismic loading which caused structural cracking, thus affecting the overall performance of the bridge [9]. This gives some indication that the diaphragm was playing a vital role in the structural load distribution. Previous studies had also concluded that the stiffness of the diaphragm could influence the strain of the bridge girder and its distribution factors among the girders. Bridges with ID had magnified significantly the distribution factor of the girders up to 25% and can also reduce the lateral horizontal force among the shear connectors in steel bridges [10]. However, in this study, the full depth of the diaphragm was adopted as a constant parameter since it was established to reduce the maximum strain on the girder compared with the partial depth of the diaphragm [11]. The aims and objectives of this study are as follows: (1) To determine whether the current level of vibration caused by the daily traffic load is affecting the serviceability of the existing concrete bridge, (2) To establish a numerical model of the concrete bridge deck based on the field measurement vibration data for dynamic assessments, (3) To identify, in accordance with code of practice recommendations, the ideal size of the intermediate diaphragm for managing the dynamic response magnitude (vertical acceleration and frequency), (4) To carry out a parametric analysis taking into account the influence of the intermediate diaphragm beam on the bridge deck's vibration behaviour.

2. Effects of Vibration on Bridge Structure

It is significant to know what effects and consequences of vibration induce/incur on the bridge structure. According to the structural dynamic principle, whenever a structure such as a bridge is imposed with a dynamic or moving load, where the frequency loading is much higher than the natural frequency of the bridge, vibration phenomenon will take place being oscillated by itself. This phenomenon is sometimes dubbed as resonance, where it can be felt due to the effect from road users or pedestrians passing through the affected bridge. The vibration on the structure behaves as a ‘dancing act’ if the difference between the loading frequency and natural vibration is high. There have been multiple examples documented about the possibility of vibration approaching the bridge endangering the comfort of bridge users. [12], [13]. When this vibration event was repeatedly triggered without any corrective action, the bridge eventually failed and collapsed, reaching a catastrophic level. [12], [14]. Additionally, a bridge that is vibrating continuously is prone to undergo fatigue, which leads them to continue deforming significantly. This issue could cause a structure to be unable to withstand the specified loadings due to a lack of elastic capacity. [15], [16]. It has been researched and proven that vibrations can move an elastomeric rubber bearing from where it is meant to be. For beam-to-slab bridges, this frequently occurred. [17]–[19]. This information is sufficient to make us aware of the vibration concern and to raise the alarm that it has to be addressed to prevent future catastrophic failures. Further, this vibration may be caused by the bridge's pier and deck slab shaking, which caused other attached auxiliary components including rail steel, expansion joints, and road signage to move away from their positions on the bridge. [19]–[21]. Additionally, vibration, especially for beam slab bridges, may cause expansion joints to make unwanted noise in addition to causing localised stress on bridge girders that are subject to wheel loads. [14], [17], [18], [20].

2.1 Factors of Vibration Generation

In dynamic principle, if the excitation frequency is more than the natural frequency of the object, the structure will oscillate or vibrate, which is also known as resonance. During this resonance, the vibration amplitude is at maximum level [22], [23]. As for external factors, there are many causes for the structure to vibrate. One of them is due to the thin depth dimension which it may result the structure becoming ‘soft’ and flexible. If there is much flexibility, the structure is prone to excessive deflection and also the frequency of the structure becomes lesser [12]. Based on Eq. (1), frequency is a function of the structure stiffness, given as:

$$\text{Frequency}, f = \frac{1}{2\pi}\sqrt{\frac{k}{m}} \quad (1)$$

where k is structure stiffness and m is the mass of the structure.

Another external factor for the bridge structure to vibrate is due to the dynamic loading carries by the traffic load. These dynamic loading that generates vibration includes braking of the vehicles, skidding force, speeding of the vehicles and vehicle cornering when taking the curvature of the road alignment. In addition, human motion such as walking or running in mass crowds could also contribute to the vibration of the bridge. Strong wind known as the sway-effect is also contributing to the vibration of the bridge. Structure deterioration such as cracks may contribute to vibration due to the change in the structure system from stiffness and mass reduction [12], [24]. This will in time modify the frequency characteristic of the structure leading to excessive deformation. It has been studied by previous researchers [25]–[28]that the damping of structure material does affect the performance of the structure towards loading excitation. The following Eq. (2) gives the relationship between material and damping magnitude:

$$\text{Damping, } \xi = 2\sqrt{KM} \tag{2}$$

where K is structure stiffness and M is the mass of the structure

If the structure stiffness or mass is high, then the damping magnitude would be high. The damping effect can make the structure more resistant to external force [16]. Eq. (3) from the new Raphson equation also known as the motion equation explained the relationship between damping and external force:

$$M\mathrm{a} + Cv + Kx = F(t) \tag{3}$$

Where M is the mass of the structure, a is gravitational acceleration, C is the structural damping, V is structure velocity, K is structure stiffness, x is the displacement of the structure due to external force and $F(t)$ is the external force.

The application of rubber bearing on the beam-to-slab bridge is another factor that contributes to the vibration on the bridge structure. Studies done by Tsubomoto et. al. [17] and Kawatani et. al. [25] found that having elastomeric rubber bearing in a bridge resulted to more vibration in the superstructure if it is designed with high damping material. Besides that, rubber bearing able to change the natural frequency of the bridge, thus influencing the vehicle bridge interaction [30]. There are many beam-to-slab bridges using this bearing device for accommodating horizontal movement due to the expansion and contraction of the bridge, especially at the beam structure. Roadway imperfection factor contributing to vibration issue is very straightforward to be comprehended because it can be visualized and observed directly. If the road quality is poor, drivers can directly feel more vibration to the car driving onto these improper road surfaces [22].

3.0 Significance of Study

The importance of this study is to investigate and comprehend the effect of the intermediate diaphragm on the vibration control of the bridge deck concerning the parametric study. The vibration outputs are acceleration and natural frequency. These outputs are important parameters for vibration measurement which had been stipulated in most codes of Practices (refer to Table 1 and Figure 1). Bridge vibration is generated primarily from the wheel load of moving vehicles. This wheel load can either be acted as a series of point loads between the girders or positioned directly onto the girder itself so that it can be deflected or rotated about its axis and hence vibrate elastically.

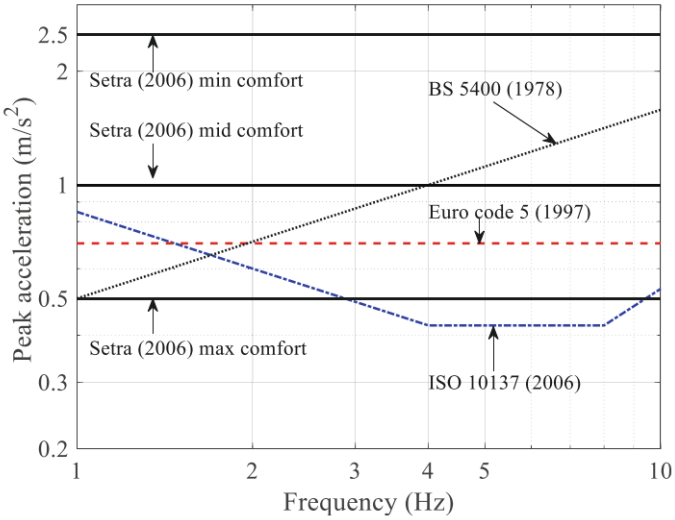

Figure 1. Acceptability of vibration in codes for bridges [31].

Table 1. Approaches to serviceability design [32].

Approaches to Serviceability Design						
Frequency Tuning Approach		***Vibration Limit Approach***				
Design Code	***Avoidance range in vertical direction (Hz)***	***Design Code***	***Satisfactory fundamental frequency minimum value (Hz)***		***Limits on accelerations (m/s^2)***	
			V[c]	**H[d]**	**V[c]**	**H[d]**
SIA 160 [13]	1.6 – 2.4 3.2 – 4.8	BS5400 [9]	5.0	1.5	$0.5\sqrt{f_o}$	*
AASHTO 1997 [16]	>3.0[a] >5.0[b]	Eurocode 5[e] [8]	5.0	2.5	0.7	0.5 or 0.2
CEB [14]	1.6 – 2.4 3.2 – 4.8	Eurocode 1[f] [7]	5.0	2.5	0.7	0.5 or 0.2
Japanese code (cited in [4] and [15])	1.5 – 2.3	OHBDC [17]	4.0	4.0	**	*
		CSA [18]	4.0	4.0	**	*
		Bro 2004 (cited by [19])	3.5	*	0.5	*
		ISO 10137[g] [20]	N.A.	N.A.	$0.6\sqrt{f_o}$ $1<f_o<4$Hz 0.3 $4<f_o<8$Hz	0.2
		Hong Kong [21]	5.0	1.5	$0.5\sqrt{f_o}$	0.15
		AS 5100.2 [22]	3.5	1.5	**	*

According to this mechanism action, this movement translated as rotation and deflection of the beam mainly at mid-span led to the vibration phenomenon. This vibration is also known as the dynamic response as a result of excitation load from the moving vehicles above the series of girders. Moreover, the location of the wheel loads situated eccentrically between these girders can also magnify the vibration effect. Therefore, the effective way to mitigate this vibration issue is by incorporating ID so that the torsional rigidity of the main girders may increase. At the same time, any movement or deflection of the main girders may be reduced with respect to the defined parametric study. Currently, there are no standard regulations and procedures available in any Codes of Practice and buildings manuals stipulating the methods on how ID to be ensembled into the bridge structure in terms of sizing, number of ID, location within the span and spacing between the ID (if more than one). This confirmatory procedure is essential for the Designer to arrange the specification of ID in bridge design as well as to optimize its contribution when resisting the transient loads. This study is also an attempt to fill the research gap by numerically studying the behaviour of IDs of the beam-to-slab bridge under traffic loads. Moreover, suggestions for the design in terms of location within the span, thickness and number of IDs are to be made.

3.1 Parametric Study

The parameter of ID to cater for this issue is the thickness of the ID at 300 mm which is the location of ID in the bridge deck solely at the mid-span of the bridge deck. (as shown in Figure 2).

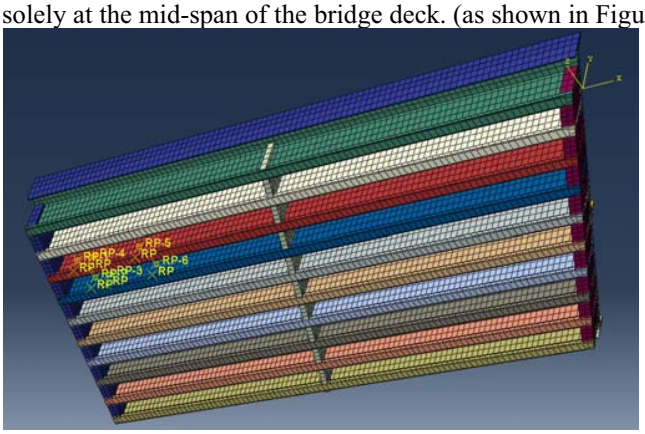

Figure 2. View of bridge deck underneath with arrangement of a single ID.

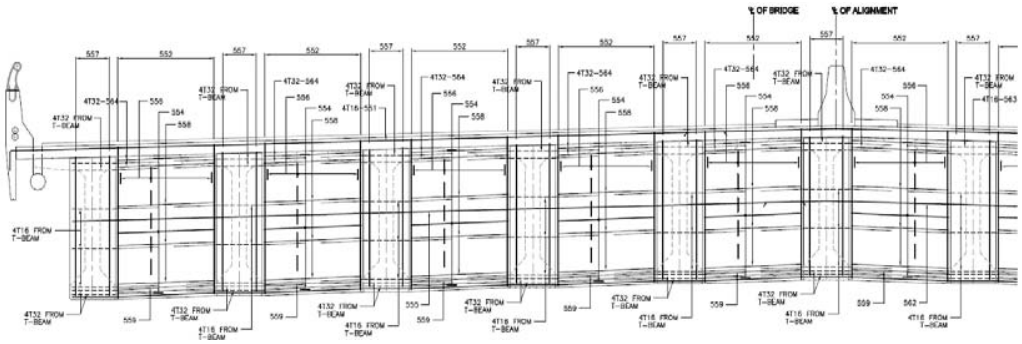

Figure 3. Typical reinforcement detail for ID.

Meanwhile, the ID depth is fixed at 2150 mm (refer to Figure 3) where same height as the girders (As shown in Figure 4).

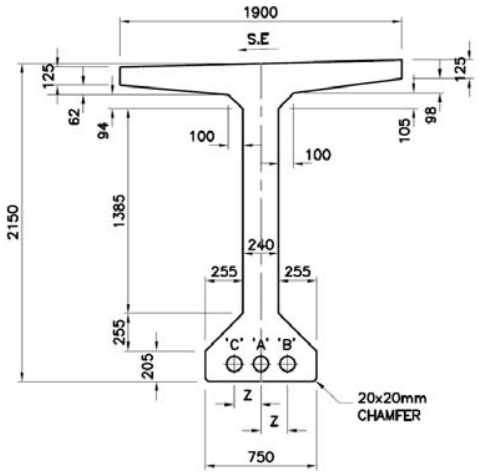

Figure 4. Dimension details of the girder.

3.2 Bridge Detail Descriptions

The entire length of the project is approximately 3 km and consists of four (4) slip-roads. Along the highway stretch, there is one area where a bridge is required to support the road alignment at two (2) routes of slip road 2 and slip road 3. (refer to Figure 5 and Figure 6).

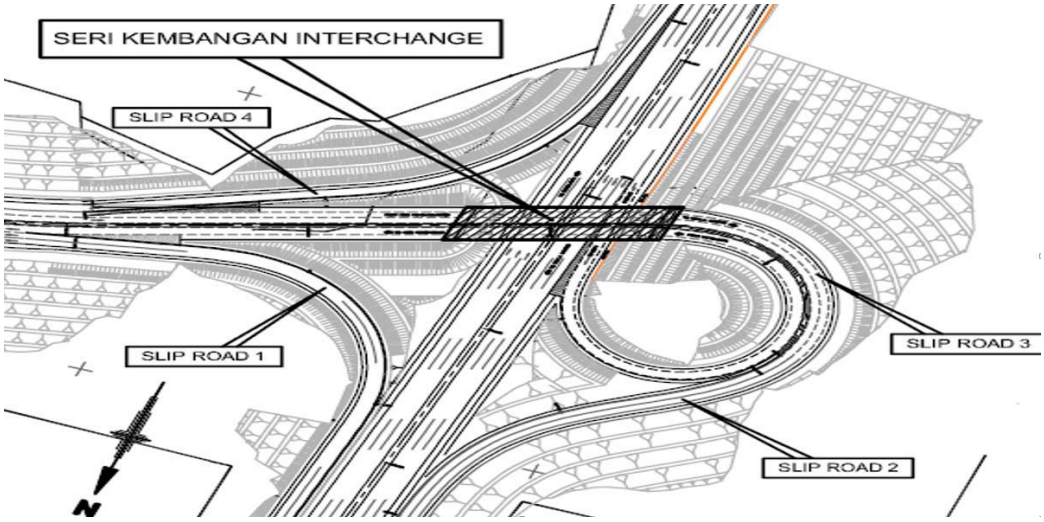

Figure 5. Location plan of the bridge.

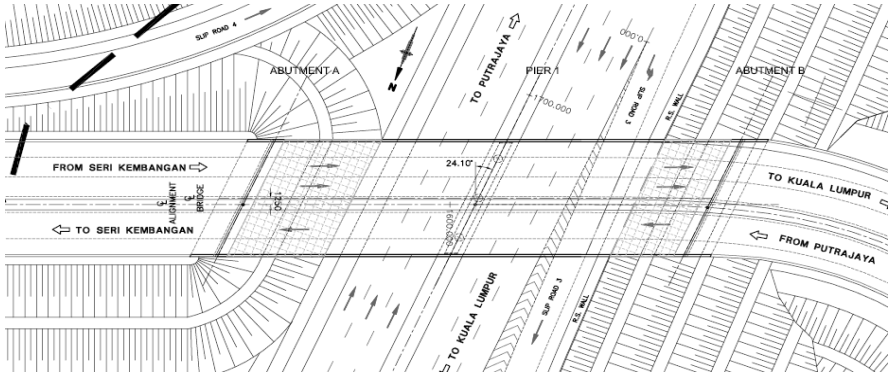

Figure 6. Bridge aerial view.

This bridge system was made featuring as in Table 2 :

Table 2: Components type of bridge system

Bridge Components	Characteristics
1. Superstructure :	
Precast concrete girder	T-beam with in-situ casting.
Girder spacing	2.20 m c/c orthogonal arrangement.
Prestressing system (VSL)	3 nos. post-tensioned (each girder) with super low relaxation (1860 N/mm^2 ultimate strength)
Strands size	7 wires of 15.2 mm diameter.
Strands wire breaking load	261 kN at the ultimate stage.
Estimated losses	22.5 % both short and long term
Humidity environment	70% - 80%.
Stressing condition	75 % of ultimate strength in 2 stages of stressing at day 7 and day 28 (transfer).
Slab	Reinforced concrete in-situ with 180 mm thickness.
2. Substructure :	
Bearing device	80 mm thick elastomer rubber bearings with 5 number of 4.0 mm steel plates. (600 mm x 350 mm).
Expansion joint at the abutment	Transflex with modular joint type.
Support system	4 number with 1.50 m diameter in-situ bored-piles at abutments and 3 number at the intermediate pier.
Pile depth	18 m – 45 m from cut-off level to toe of the pile.

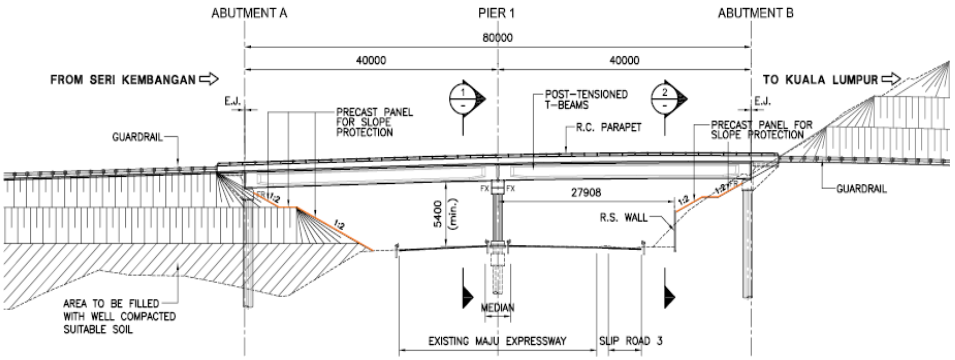

Figure 7. Elevation of span configuration of Seri Kembangan Bridge.

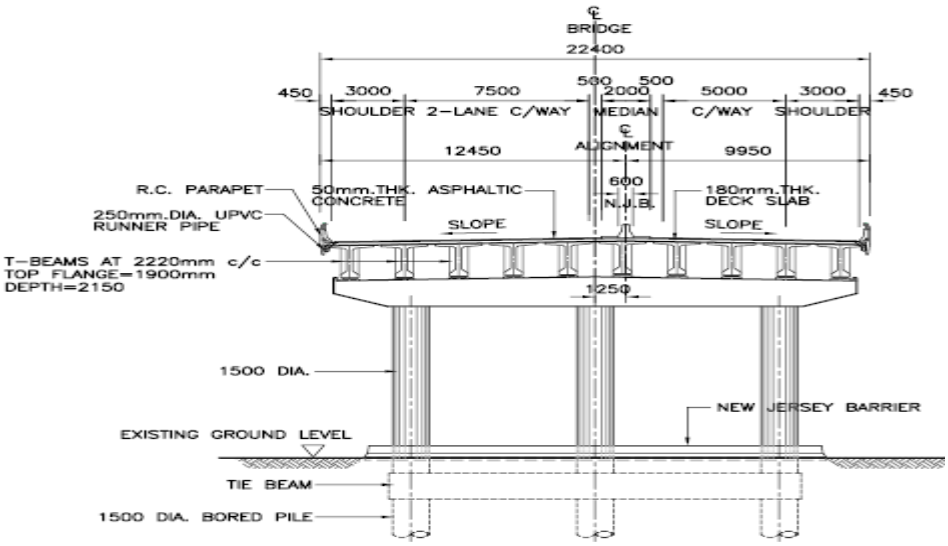

Figure 8. Typical pier cross-section.

Underneath the prestressed girders, elastomer rubber bearings with 80 mm in total thickness and coupled with resin mortar were applied to allow the horizontal movement of the RC bridge deck due to temperature and load effect (as shown in Figure 8). There are 2 nos of End diaphragms that were built for each deck span. Figure 9 shows the arrangement of the end diaphragms underneath the bridge.

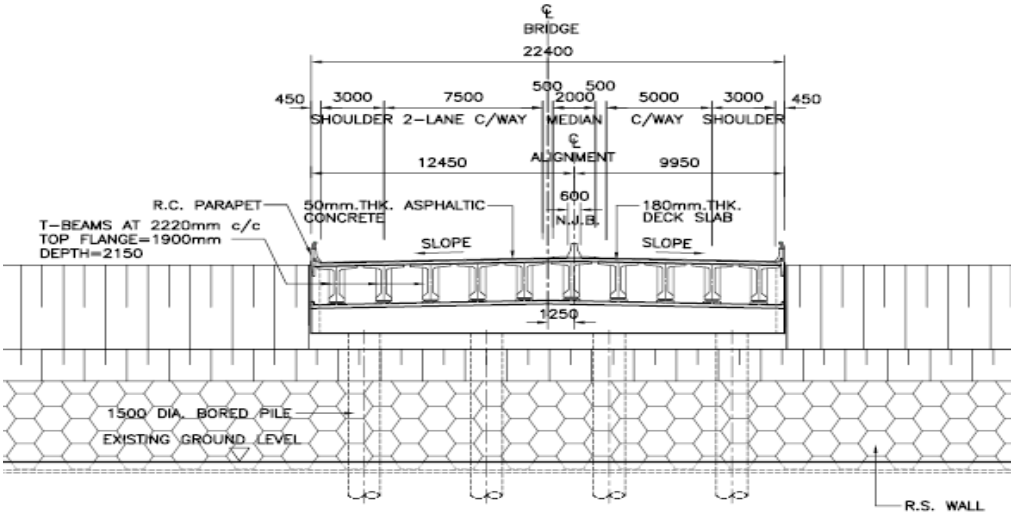

Figure 9. Typical abutment cross-section.

Figure 10. Physical view of bridge underneath.

4.0 Vehicle Bridge Interaction (VBI)

The dynamic responses of the interaction VBI system in this study is simulated using the finite element approach. The VBI system is first given the general equations of motion in a matrix form. Then, the penalty method (in contact interaction) is introduced to solve the interaction between the vehicle and the bridge. Next, to solve the equations of motion, the time integration method is presented. It is important to note that the penalty method and the time integration method are both now supported by ABAQUS. The dynamic equation for the coupled VBI system can be written as:

$$[\mathrm{M}]\{a^t\} + [\mathrm{C}]\{v^t\} + [\mathrm{K}]\{u^t\} = \{F^t\} \quad (4)$$

where *M*, *C* and *K* denote the mass, damper, and stiffness matrices of the whole system, respectively. *K* is a stiffness matrix with respect to the virtual springs between the contact parts. Meanwhile,

$\{a^t\}$,$\{v^t\}$and $\{u^t\}$ denotes the acceleration, velocity and displacement vectors of the nodes at time step *t*, respectively. Also, F^t is the external force applied to the system.

In detail, the equations of motion for a vehicle can be written in a matrix form as:

$$[M_v]\{a_v^t\} + [C_v]\{V_v^t\} + [K_{v,}]\{U_v^t\} = \{F_{bv}^t\} + \{F_{gravity}\} \quad (5)$$

where U_v^t, V_v^t , and a_v^t, denotes the displacement, velocity and acceleration vectors of the vehicle at time step *t*, respectively. Also, M_v, C_v, and $K_{v,}$ represents the mass, damping and stiffness matrix of the vehicle, respectively. $F^t{}_{bv}$ denotes the external force, which consists of the interaction force between the tracks and wheels applied on the vehicle, and $F_{gravity}$ denotes the gravity force. Interaction forces are functions of bridge responses, indicating that the vehicle's responses are affected by the bridge responses through VBIs. Similarly, the equation of motion for the bridge structure can be expressed in a matrix form as:

that the vehicle's responses are affected by the bridge responses through VBIs. Similarly, the equation of motion for the bridge structure can be expressed in matrix form as:

$$[M_b]\{a^t\} + [C_b]\{v^t\} + [K_b]\{u^t\} = \{F_{bv}^t\} + \{F_g^t\} \quad (6)$$

Where M_b, C_b and K_b, respectively denote the mass, damper, and stiffness matrices of the bridge structure. Also, a^t , v^t, and u^t respectively denote the acceleration, velocity and displacement vectors of nodes. F_{bv}^t represents the external force caused by the moving vehicle. F_g^t expresses the ground force caused by an earthquake or soil pressure applied to the bridge structure.

4.1 Limitation of Modelling

The limitations of numerical modelling for this study are as follows:

i. Limited to a simply supported bridge structure with 40 m in length for each span and the bridge deck is made of the prestressed concrete girder with the in-situ reinforced concrete slab.
ii. Modelling of the bridge elements is covered from deck slab level to elastomeric rubber bearings stiffness level since the provided piers height (5.4 m) and its diameter is considered as very stiff and categorized as short column. Hence, soil-structure interaction is neglected in this study. No continuity effect is considered between the approach slab or embankment and the span of the structure since the bridge is not designed as an integral or monolithic.
iii. Result outputs are in frequency, vertical acceleration, and displace or mode shapes.
iv. This bridge is limited to a straight span consisting of a 24.1° skew on the plan.
v. Both end and intermediate diaphragms are rectangular with a fixed height of 2.10 m.

4.2 Methodology of Finite Element Analysis (FEA) with Vehicle Element–Bridge Element Interaction

4.2.1 Type of Analysis Step. The VBI problem is solved with the presence of a numerical analysis framework in ABAQUS. There are two (2) steps defined in this modelling. The first step is known as *static with linear perturbation* which is used to capture the Eigenvalue frequencies with associated mode shapes while for second step is known as *Dynamic Explicit* analysis. For the *static linear perturbation* step, no specific time is defined since this step does not relate to the time parameter (see Figure 11). The normalized Eigenvectors based on displacement are selected to calculate the frequency and mode shape. Meanwhile, for the *dynamic explicit*, 0.003 seconds is taken as in the first stage for the stabilization

stage where the truck loading is applied gradually to avoid diverging and numerical instability. In the second stage, 9.0 seconds is taken to represent the actual time in the field test (time path length). The normalized Eigenvectors based on displacement are selected to calculate the frequency and mode shape.

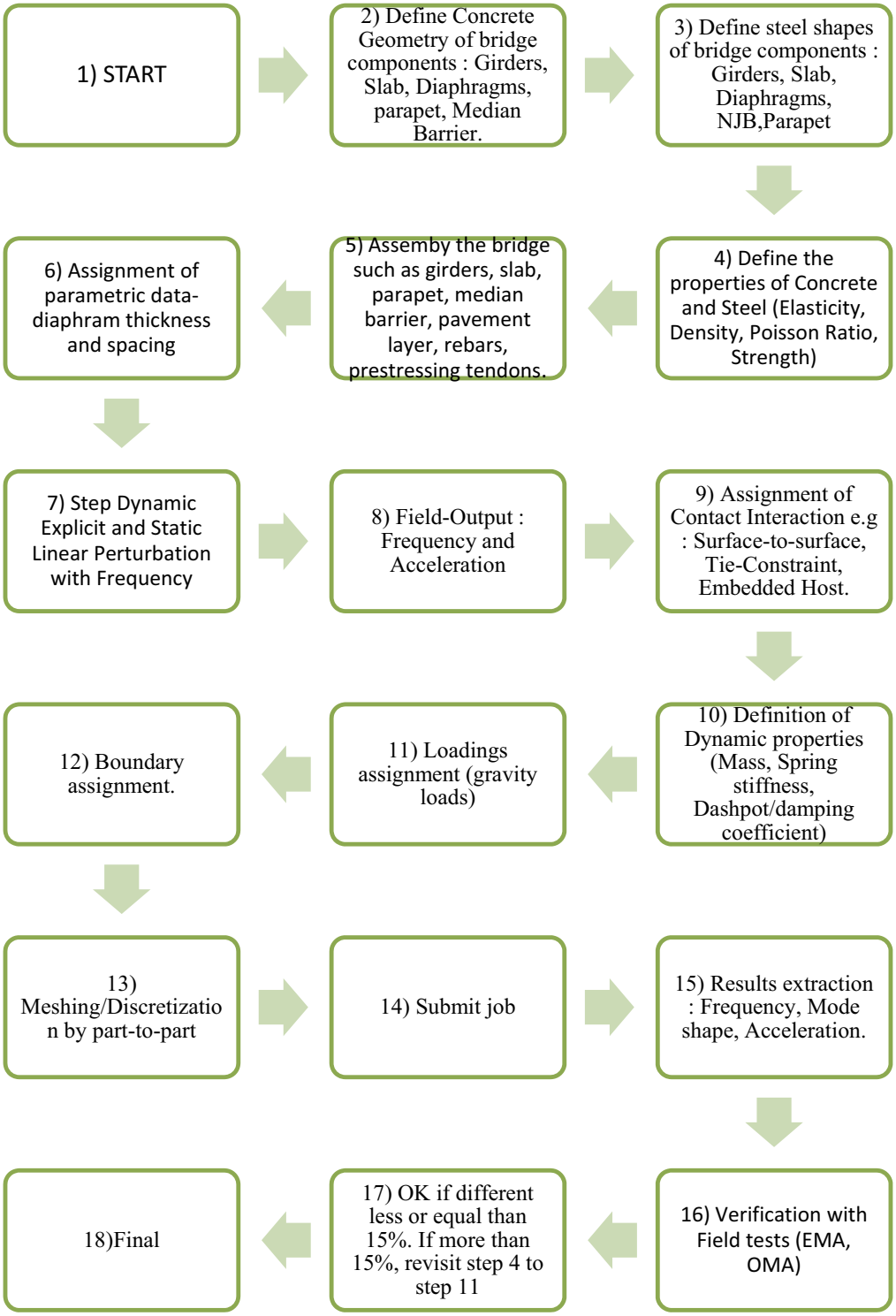

Figure 11. Methodology of numerical analysis steps.

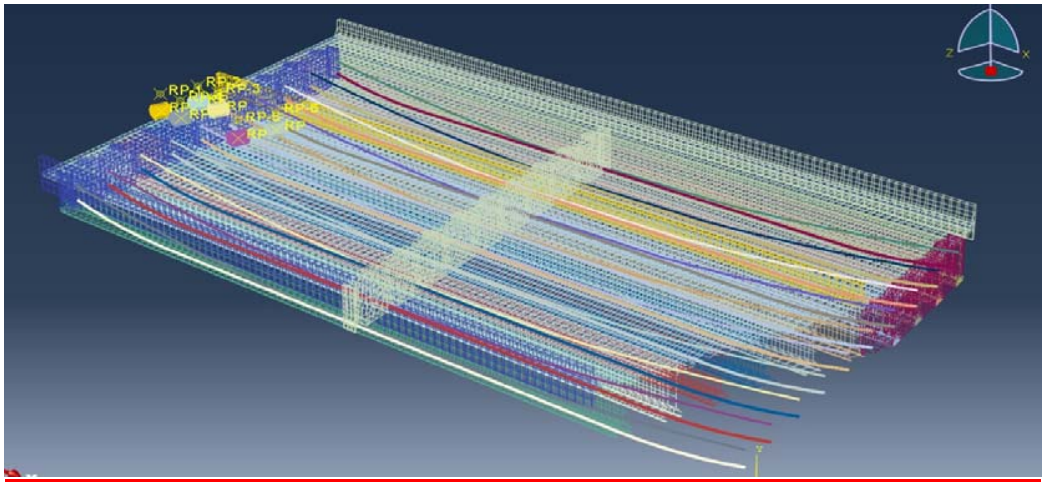

Figure 12a. Overall bridge modelling in 3D view.

The first step is also employing the frequency domain parameter to generate the Eigenvalue results. In the second step, *Dynamic Explicit* is activated using the time-domain function to calculate the bridge deck acceleration magnitude due to the moving load effect. The equation of motion (Newton-Raphson) from Eq. (3) is employed in the second step for the numerical analysis.

4.2.2. Assembly of Elements. The main components of the bridge structure are modelled as per the existing structure. Among the modelled bridge components are the girders, end diaphragms, ID and reinforced concrete (RC) slab. The road furniture such as parapets and median barriers are also included together in the bridge model since they also contribute to the overall stiffness of the bridge structure [33]. Therefore, both parapets and median barriers are modelled and integrated with the bridge structure through the monolithic action with the RC slab (see Figure 12a). This monolithic action in modelling is translated using the *tie constraint* condition. The RC slab with 180 mm thickness is modelled together with a 65 mm thickness premix. The connection between these two elements is created using the *tie constraint* type. The rigid wheels (outer tyre diameter: 1117 mm, wheel outer diameter: 918 mm) are added to the model to simulate the contact between the wheel load and the bridge deck. The spring-mass and the bridge structure (girders, parapets, median barrier, slab, and premix) are modelled with an eight-node brick element with enhanced hourglass integration (C3D8R) solid elements. The wheel is simulated with a rigid body (non-deformable) and modelled using C3D8R elements. Meanwhile, prestressing steel elements are modelled using truss elements in 3D. A pre-defined field with a stress parameter is used with 75% of the ultimate strength and activated in both vertical and horizontal vector forces to represent the prestressing force in the girders. The embedded and host regions are defined for prestressing steel and girder contact (refer to Figure 12a). Similar approach is applied for other steels (*main rebars and stirrup*) and concrete components (*parapet, median, RC slab*). A 10-wheels unit is modelled representing the 24 tonnes 10-wheeler truck (refer to Figure 12b). This is then followed by the actual configuration dimension of the truck.

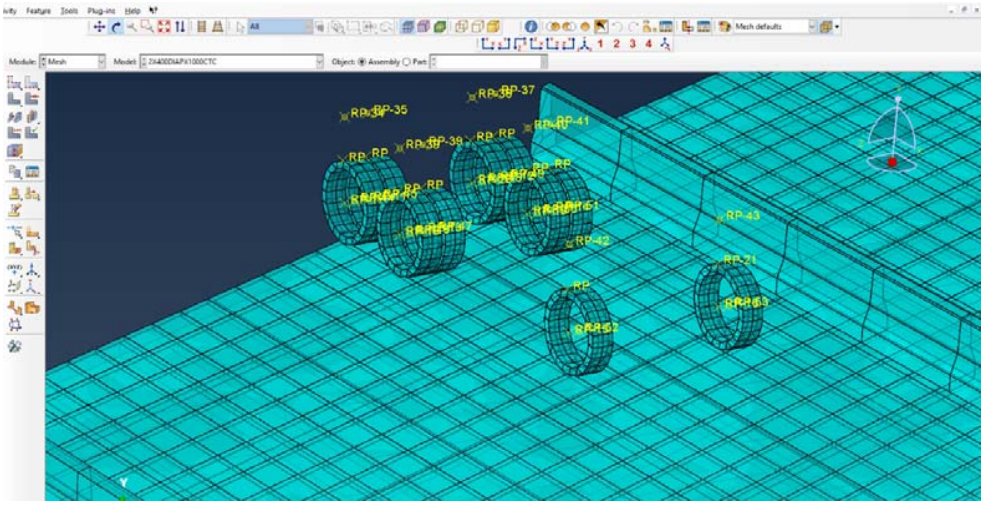

Figure 12b. Vehicle bridge modelling in mesh mode.

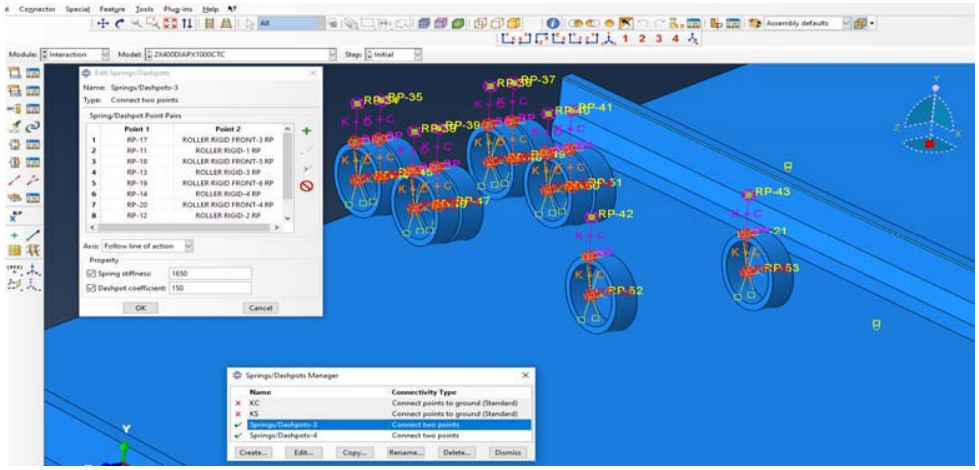

Figure 13. Spring dampers are installed based on the actual condition.

4.2.3. Elements and Meshing Setup. The elements or global seeds size varies from 20 mm to 1100 mm with C3D8R (8 nodes linear brick) as the main element type. For time-saving, a mass scaling approach with a *12 multiplier* is adopted by ensuring the *kinetic energy* is lesser than *internal energy*. The spring-mass and the wheels are connected with a spring between their centre of mass (Fig. 12b and 13). The type of 3D-*hexagon* (*stress*) with the function of hourglass enhanced is utilised for all bridge components as a core element in this modelling. The *linear geometric order* for all elements is used in both 2 steps of analysis. The *reduced integration* function is activated to obtain a good result estimation.

4.2.4. Contact Interaction. Interaction between the wheel and the bitumen top surface consists of the surface-to-surface type where a friction coefficient, $\mu = 0.6$ is (as depicted in Figure 14) applied [25]. The main contact formulation includes three (3) aspects: normal behaviour, tangential contact and hard contact (a rigid surface is assumed for the top girder).

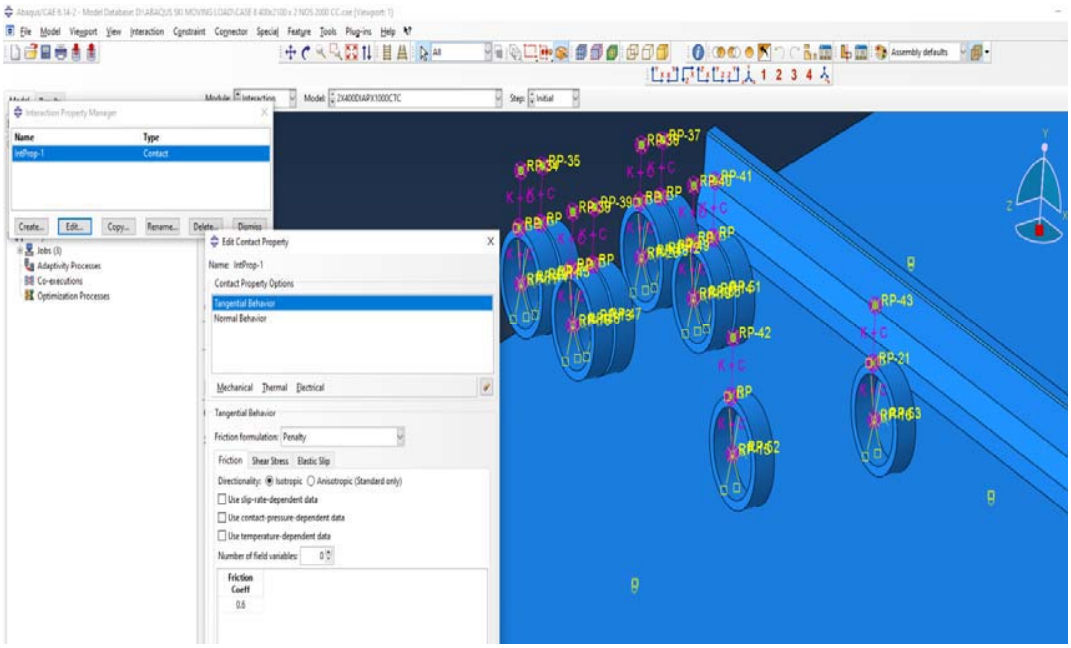

Figure 14. Contact interaction input.

The connection between the nodes and regions is based on the contact discretization principle. The connection between nodes and regions might alter over the periods because of the truck movement. While the changing interaction between elements (tyres and road pavement) may involving of deformation, penetration, and separation. [34]. To determine the contact nodes and regions for each time step, the “surface-to-surface contact" setting was selected. Two surfaces were predefined in pre-processing of the model before the submission of the job where the top of the beam (designated as a master surface since it is a supporter) and the wheel was designated as a slave surface condition. Potential contact regions were chosen in this contact pair. Adjacent nodes on the slave surface are projected on the master surface to form “node-to-surface" contact pairs. The surface-to-surface contact considers both the master structure (concrete deck irregularity) shape and the slave structure (wheel) shape and averages the contact condition to raise the pressure accuracy. [34]. In the normal direction, the “hard" contact” relation was selected to minimize penetration. ‘Penalty" method was selected for the “constraint enforcement" option. Related parameters of the penalty method are represented as the setting of virtual spring stiffness in the contact regions. In this procedure, Newton–Raphson iteration is used to solve dynamic equations as given in Eq. (3) and Eq. (4).

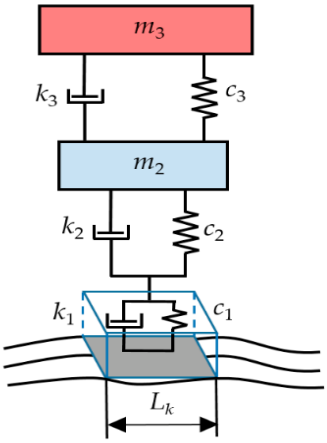

Figure 15. Quarter-car model: Lk—tire-road contact length; m1, c1 and k1—mass, stiffness, and damping ratio of the tire tread part; c2, k2—tire stiffness and damping ratio; c3, k3—suspension stiffness and damping ratio; m2—unsprung mass; m3—sprung mass. [35].

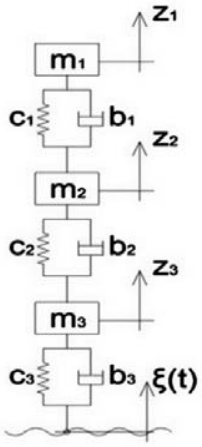

Figure 16. Example of Linear Oscillatory Model of the vehicle [25].

4.2.5. Mass, Spring Stiffness and Damping

In the assignment of vibratory property for moving load, the mass and stiffness coupled with damping values are assigned to the wheel of the truck. This idealisation is based on the Dynamic principle (Single Degree of Freedom or SDOF) and previous studies [25], [35](see Figure 15 and Figure 16). All the properties have been used based on the manual such as tyre stiffness, absorber stiffness, and damping values [35]–[41].

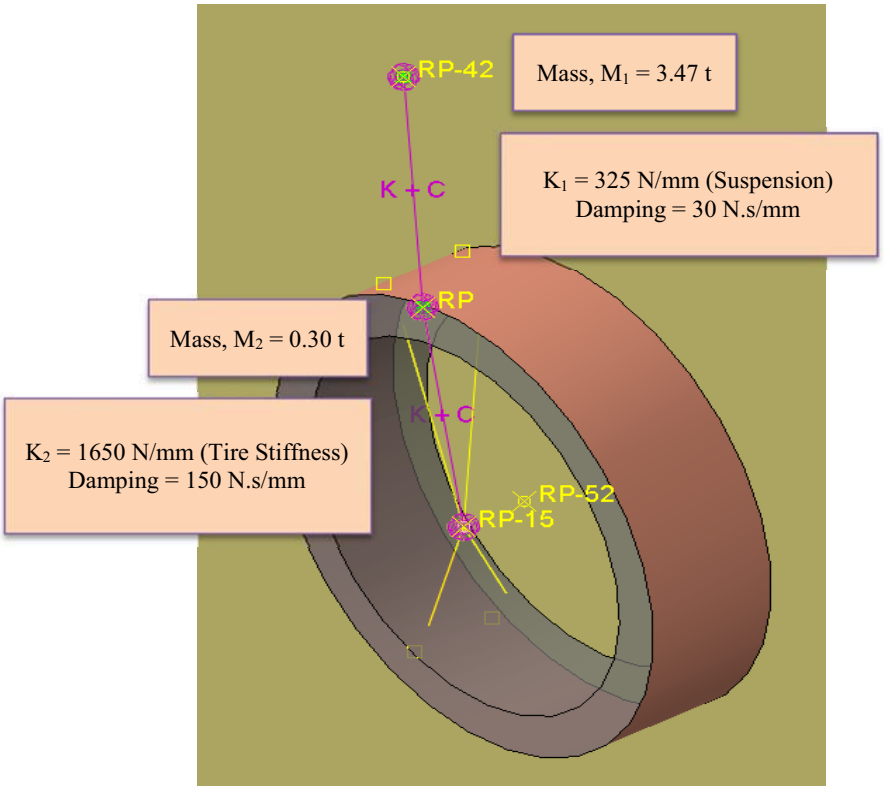

Figure 17. Linear Oscillatory Model of the 24 tonnes lorry for this study (Front wheel).

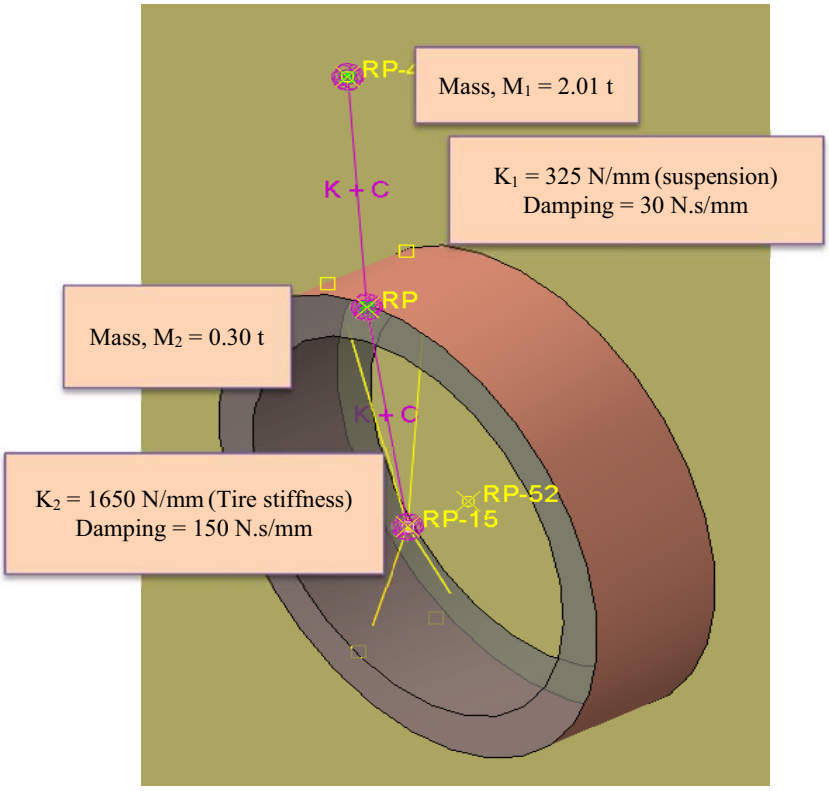

Figure 18. Linear Oscillatory Model of the 24 tonnes lorry for this study (rear wheel).

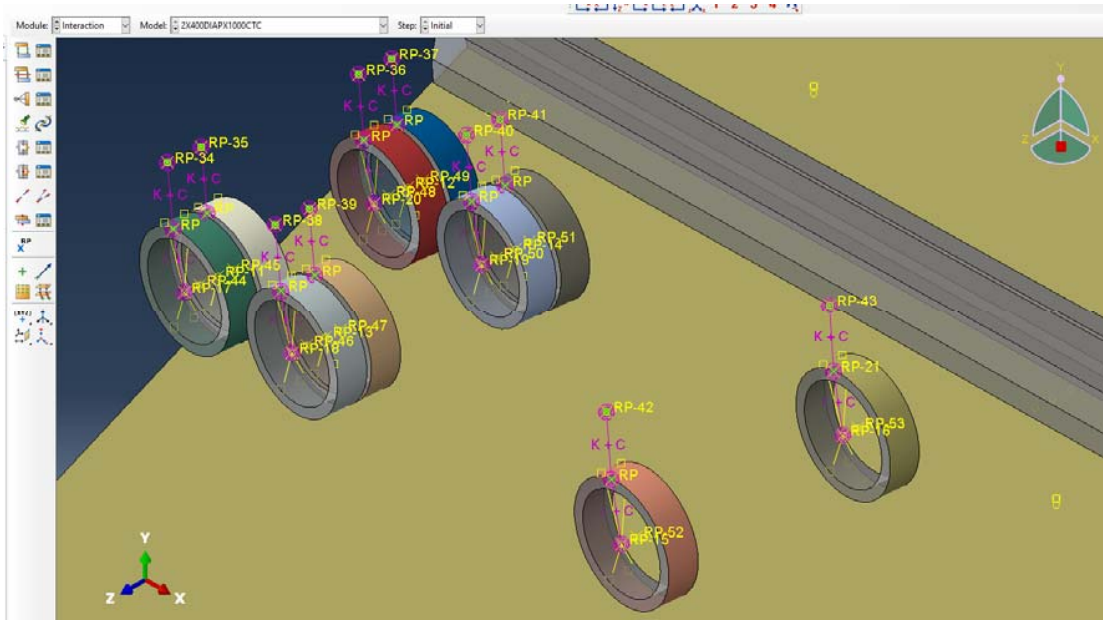

Figure 19. Wheels arrangement in modelling.

4.3. Construction of Bridge Materials

In the modelling stage, the material properties of the bridge components are defined based on the actual materials used during the construction. This approach is taken into consideration so that the error between the numerical analysis (modelling) and field results is within the limit. Table 3 shows the properties of each bridge material.

Table 3. Material properties of the bridge structure components.

Materials	Components	Strength (N/mm^2)	Elasticity (kN/mm^2)	Density (kN/m^3)	Poisson ratio, ν
Concrete	RC Slab	40	32	25.00	0.1
	New Jersey Barrier/Median	30	30	25.00	0.1
	Girder	60	34	25.00	0.1
	Diaphragm	40	32	25.00	0.1
	Pier	40	32	25.00	0.1
	Pile Cap	40	32	25.00	0.1
	Bored Pile	40	32	25.00	0.1
Steel	High Yield Rebar	460	195	78.60	0.3
Prestressing Strands	7-wire Strands Low Relaxation Type (15.2 mm dia)	1860	195	78.60	0.3
Bitumen	Overlay with 50 mm thick	10	4	23.00	0.4

4.4. Loadings

There are several primary loads have been considered in the numerical modelling. These loadings are estimated following the actual loadings that are applied to the bridge structure. The following details are descriptions for each load component:

Imposed Load: A moving wheels load consists of 3-axles (10 tyres) lorry weighted 24 tonnes (Figure 20a) with sand filling material is mobilized to induce the force vibration for the *Operational Modal Analysis (OMA)* test. This load configuration is selected because of its high availability on most highways in Malaysia. In addition, the spacing of the axles is considered quite close to create a high-intensity pressure load between the tyres and the road due to the overlapping of the load dispersal.

Figure 20a. Force vibration test (Operational Modal Analysis-OMA).

Superimposed Dead Load 1: These loadings consist of granular material such as road pavement. The pavement with 65 mm thickness and its properties as shown in Table 3 are defined in the Abaqus loading menu and calculated automatically during the analysis.

Superimposed Dead Load 2: This load for the road furniture such as concrete parapets and median barrier are derived based on the actual detailed dimension. All the material properties such as concrete density, Elastic Modulus and Poisson's ratio are stipulated in Table 3 and applied for calculation in the analysis stage.

Excitation Force: This load is used for *Ambient Vibration Test (AVT)* simulation to exert the impact or impulse force on the structure. This impact force is generated by knocking the concrete deck with the modal hammer which in turn to excite the bridge deck response (see Figure 20b). This response will be processed based on the frequency response spectrum wave. Next, the process to identify the natural frequency of the bridge as well as mode shapes through signal processing of electric device known as *Data analyser-DAQ.*

Figure 20b. Hammering of excitation points for the modal test (also known as Experimental Modal Analysis-EMA).

Dead Load: The self-weight of bridge structures such as RC slab, girders, diaphragms and rebars are calculated according to the actual 3D object and the density of the given materials in the modelling. This 3D object is modelled in full-scale measurement. The densities of the object (Table 3) are defined and activated through the gravitational load menu.

Prestressing Force: The active force is activated by defining the predefined field –stress in the vertical and lateral direction. These forces consisted of 3 prestressing tendons stress with a total of 8245 kN after losses.

4.5. Boundary Conditions

All modelling of the bridge was following the actual boundary conditions. In general, this 2-span bridge has been pinned at the intermediate pier by adopting the dowel bars which this dowel protrudes from the concrete pier head and are embedded into the end diaphragm of both spans (see Figure 6). These dowel bars are acting as stoppers for deck movement horizontally but another support on both abutments will be assigned as free to move in all directions. A similar approach has been applied in Abaqus modelling where one side of support is pinned and another support is free. Rubber bearing stiffness and damping have been neglected for this modelling since their effect is minimum [42].

5.0 Verification of Results and Discussion

5.1. Frequency and vertical acceleration results

The following figures (see Figure 21, Figure 22a, Figure 22b, Figure 23a, Figure 23b, Figure 24a and Figure 24b) show results of frequency along with respective mode shapes and vertical acceleration results of the bridge deck. These results are being generated based on a case-by-case basis for example with the parametric study that was determined earlier. Technically for modal test on-site, the displace/mode shapes of the longitudinal centerline of the bridge (single line) were used to compare with the median barrier element in numerical modelling. This approach was thought since the central longitudinal single line adjacent to the median barrier was a relevant element for purpose of comparison with the median barrier in modelling. Meanwhile, for acceleration results, the centre point at the mid-span of the bridge length was the target location for the measurement of the result. The main parametric study by incorporating different sizes of diaphragm width and location with different diaphragm spacing was investigated to identify the response of bridge structure in terms of dynamic behaviour such as frequency and mode shape features. According to BS 5400 part 2:1990 [31], [43], the minimum bridge frequency shall be designed is 5.0 Hz. While for vertical acceleration, the upper limit of 1.5 m/s^2 shall not be exceeded. This regulation is stipulated to warrant the comfortability of road users as well as to maintain the serviceability of bridges in terms of fatigue effect and excessive stress (local stress). According to the current measurement on the existing bridge deck *(OMA test)* coupled with the modal test (AVT), the generated result of vertical acceleration is not exceeding the upper limit of the code of practices *(BS5400 part 2: 1990)*. However, for first-order frequency, it is shown that the existing frequency reading (3.92 Hz) is less than the minimum frequency (5.0 Hz) required by the code of practices [13], [22], [31], [44]–[46]. This anomaly result (frequency) could trigger some fear of detrimental effect (leading to resonance due to time-dependent deformation against daily traffic loading) to bridge engineers who anticipated that bridge might last up to 120 years without any fatalities to take place. Verification works have been made through the two dynamic tests *(Modal test and OMA)* to confirm the accuracy of this numerical analysis study. This verification by field experimental is needed to be done to ensure all the parameters values that were assumed *(Concrete Elasticity, Steel elasticity, strength of materials, Poisson ratio and densities*) are in the right values and order. Generally, the results different are not so significant. For example, the acceleration and frequencies (First, Second-order and Third mode) are quite similar between field results and FEA results. This minor anomaly or error might happen due to several factors such as accelerometer units need more numbers for signal detection purposes (smooth shapes), the accelerometer was not to be mounted securely, ambient vibration due to low wind speed, and affected of some disturbance from personnel movement at adjacent on-site measurement. These are possibilities that were expected gave an affect the data collections on site.

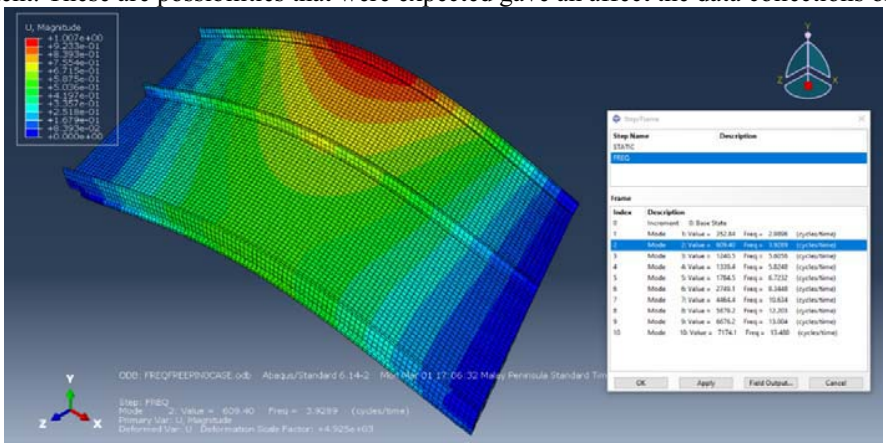

Figure 21. Frequency (3.92 Hz) and mode shape of the existing bridge structure (First Mode shape in 3D view).

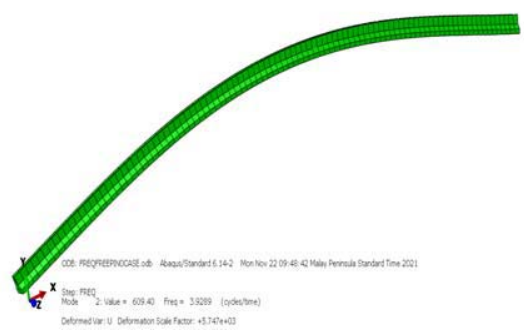

Figure 22a. First Bending Mode shape (3.929 Hz) based on numerical analysis (Abaqus).

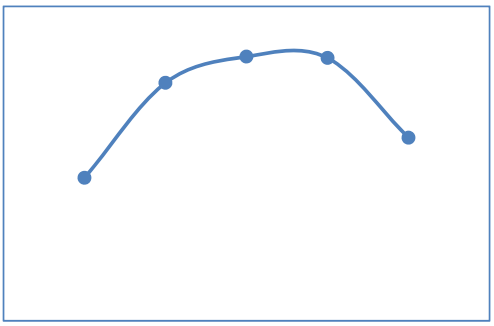

Figure 22b. First Bending Mode shape (3.921 Hz) based on Modal Testing (Experimental).

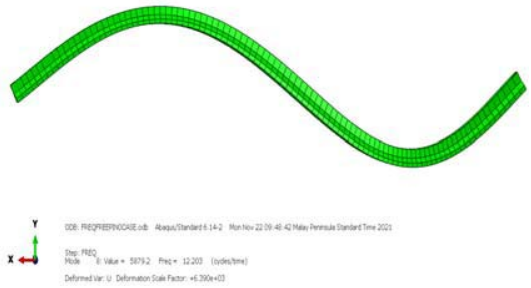

Figure 23a. Second Bending Mode (2nd Order) shape (12.203 Hz) based on numerical analysis (Abaqus).

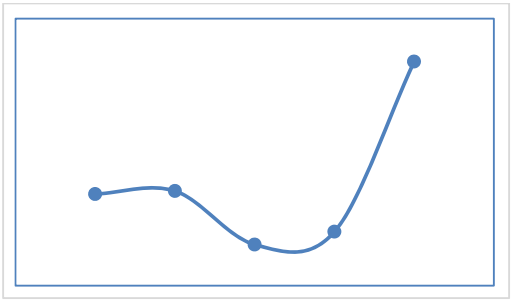

Figure 23b. Second Bending Mode (2nd Order) shape (12.207 Hz) based on modal testing (Experimental).

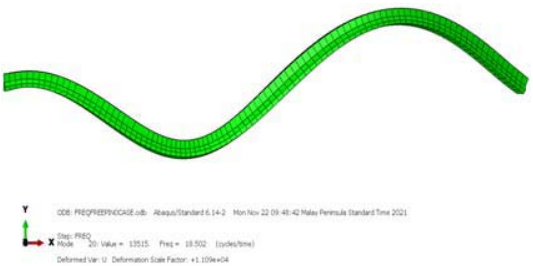

Figure 24a. Third Mode (3rd Order) shape (18.502 Hz) based on numerical analysis (Abaqus).

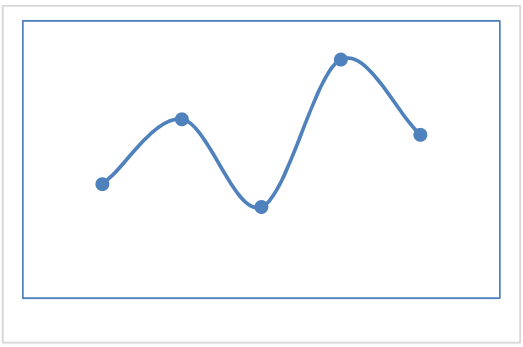

Figure 24b. Third Mode (3rd Order) shape (18.555 Hz) based on modal testing (Experimental).

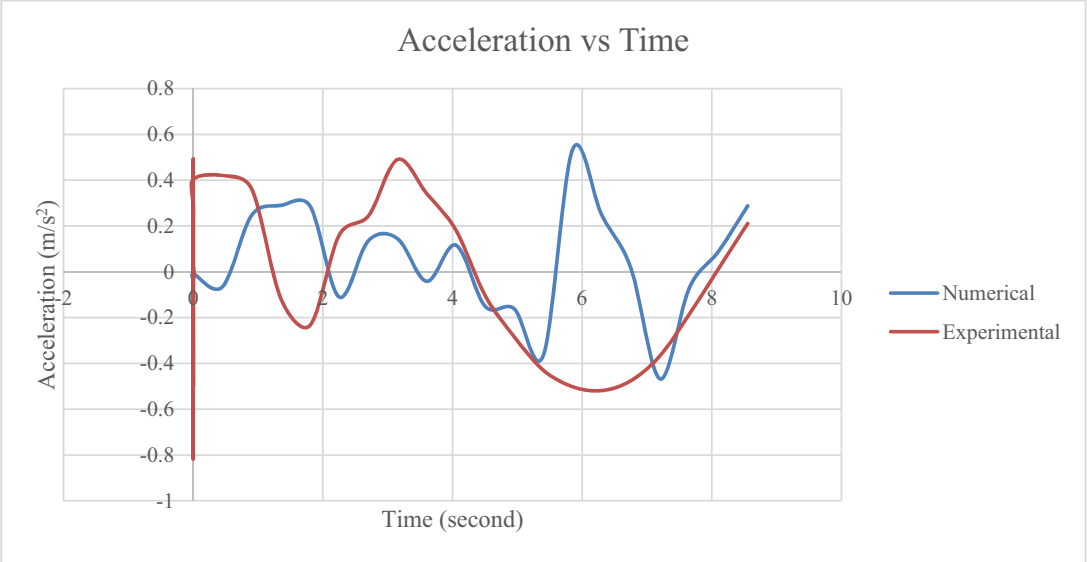

Figure 25. Comparison of accelerations between numerical and experimental.

Table 4. Results of accelerations between numerical and experimental.

Outputs	Experimental	Numerical	Error
Acceleration (m/s2)	0.490	0.534	8.98 %

5.2. Finite element analysis results and findings

The following figures (refer to Figure 26, Figure 27, and Figure 28) have shown some predictions and results based on numerical calculations. This numerical analysis is generated according to adjustment of design parameters *(Densities, Elasticity, stiffness, damping*) with taking account of the actual results from field tests earlier. From these results, the findings of the study can be written as below:

1. In general, it is observed that the presence of ID in bridge structures can affect the response of the structure in terms of acceleration values as a result of traffic loading. This can be seen from the graph results (as depicted in Figure 26) that the difference between the before and after modification of the bridge was made by inserting the ID.
2. The FEA result shows (Figure 26), that by placing the ID at the mid-span of the bridge deck, the deck acceleration was reduced up to 59.63 %. This reduction is considered such as of tremendous amount.
3. The acceleration of the bridge deck (Figure 26) in the existing condition is categorized as under the upper limit of codes (BS5400 part 2: 1990) requirement which is 0.534 m/s^2 (as shown in table 4) lesser than 1.5 m/s.
4. Referring to Figure 27, the result was shown the natural frequency of the bridge has increased from 3.29 Hz (without ID) jump up to 4.57 Hz. This positive change gives to 38.91% increment which is close to the minimum 5.0 Hz requirement by codes [13], [22], [31], [44]–[46].
5. It is indicated that ID with the 300 mm thickness located at mid-span not complying with the code regulation for minimum frequency (as shown in Figure 28) shall be attained to avert the excessive vibration. However, the presence of ID on the bridge deck has increased the existing

natural frequency of the bridge (as depicted in Figure 26, Figure 27 and Figure 28) from 3.29 Hz to a minimum of 4.57 Hz. This result is in line with equation (1) and equation (3).

Figure 26. Acceleration magnitude according to ID spacing and ID thicknesses.

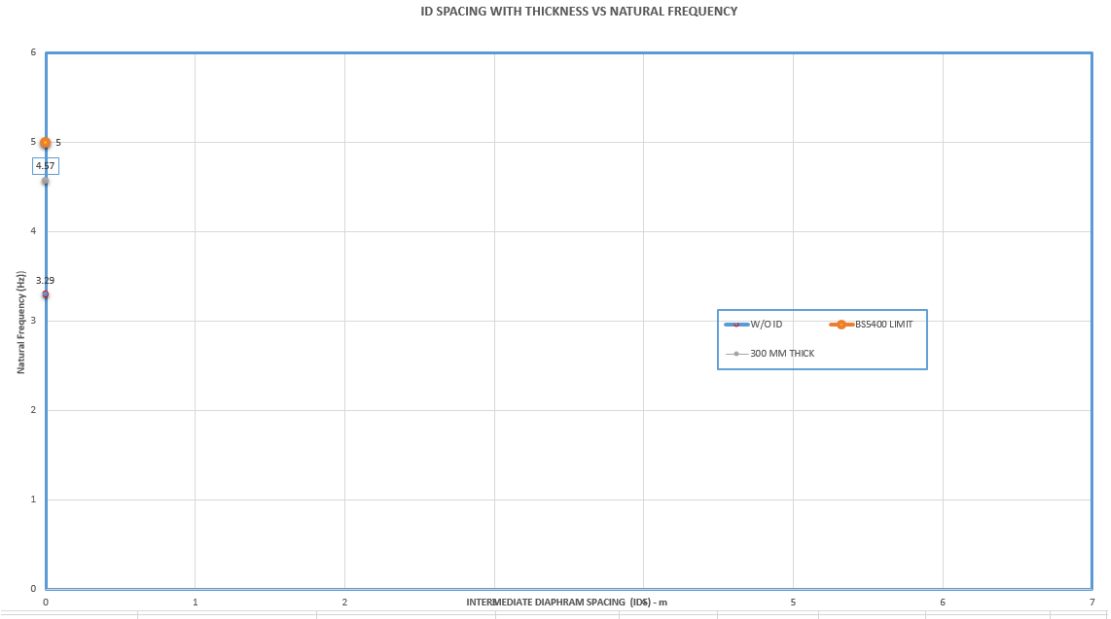

Figure 27. Bridge frequency magnitude according to ID spacing and ID thicknesses.

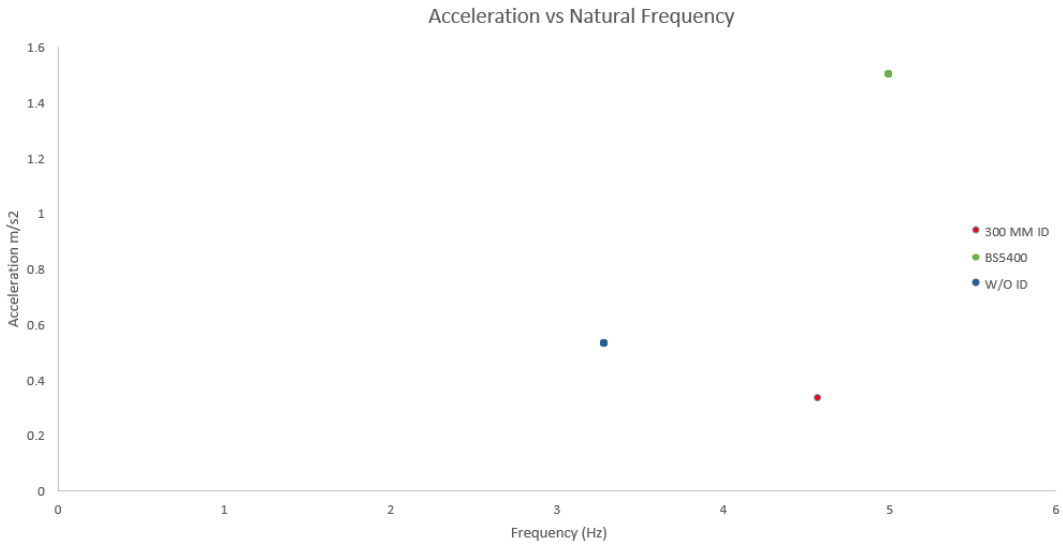

Figure 28. Bridge acceleration against natural frequency in respect to the parametric study.

6.0 Summary and conclusion

In this research paper, the results of numerical analysis based on a parametric study basis were discussed and the following conclusions can be drawn:

1. Intermediate diaphragm (ID) with full depth is giving effect towards both acceleration and frequency in terms of the degree of magnitude since it was contemplated to have the high torsional rigidity. This gives some clues that ID may influence the load live load distribution on the bridge deck as well as vibration mode (displacement shape) which is giving clues for those who do not contemplate the usage of ID in bridge construction.
2. With the ID of 300 mm thickness and located at the mid-span of the deck, ID can reduce the deck acceleration significantly the magnitude of acceleration when compared to the bridge deck without any ID in the span of the deck (As depicted in Figure 26 and Figure 28).
3. Based on the graph results (as depicted in Figure 27), it was concluded that ID can increase the frequency of the bridge which could improve the stiffness and ultimate capacity of the bridge. This increment is quite significant to barrier the bridge structure away from resonance.

4. By having these clues or results, it is imperative in beam-to-slab bridge construction particularly long and slender spans of beam slab bridges to incorporate the ID at least a single ID at the centre of the span for bracing and stiffening the deck from excessive vibration due to high volume traffic loading presently as well as sway effect due to accidental and braking load by vehicles.
5. It is alarming to bridge design practitioners from this study to control the deflection and rotation of girders due to the eccentric wheels load by putting the ID within the span so that the elastic vibration effect can be reduced and improved.
6. It is a wrong interpretation to conclude that ID does not have an impact on stiffening the bridge deck since both frequency and acceleration results were improved in complying with the code regulations although to a modest effect.

Acknowledgement

The authors would like to send their warmest appreciation for the technical supports from the School of Civil Engineering, Faculty of Engineering, Universiti Teknologi Malaysia and the financial research support by Universiti Teknologi Malaysia and Hanyang University Korea, No. R.J130000.7309.4B688. The author also would like thanks to Maju Expressway (MEX) Sdn. Bhd. and HSS Engineers Bhd. (HSS Integrated) for their support and assistance in this research.

References

[1] C. S. Cai, M. Araujo, A. Chandolu, R. R. Avent, and W. Alaywan, "Diaphragm Effects of Prestressed Concrete Girder Bridges: Review and Discussion," *Pract. Period. Struct. Des. Constr.*, vol. 12, no. 3, pp. 161–167, 2007, doi: 10.1061/(asce)1084-0680(2007)12:3(161).

[2] A. Chandolu, "Assessing the Needs for Intermediate Diaphragms in Prestressed Concrete Girder Bridges ," 2005.

[3] A. A. Semendary, E. P. Steinberg, K. K. Walsh, and E. Barnard, "Live-Load Moment-Distribution Factors for an Adjacent Precast Prestressed Concrete Box Beam Bridge with Reinforced UHPC Shear Key Connections," *J. Bridg. Eng.*, vol. 22, no. 11, p. 04017088, 2017, doi: 10.1061/(asce)be.1943-5592.0001127.

[4] M. S. Cheung, R. Jategaonkar, and L. G. Jaeger, "Effects of Intermediate Diaphragms in Distributing Live Loads in Beam-and-Slab Bridges.," *Can. J. Civ. Eng.*, vol. 13, no. 3, pp. 278–292, 1986, doi: 10.1139/l86-040.

[5] Q. V. Vu, D. K. Thai, and S. E. Kim, "Effect of intermediate diaphragms on the load – carrying capacity of steel – concrete composite box girder bridges," *Thin-Walled Struct.*, vol. 122, no. October 2017, pp. 230–241, 2018, doi: 10.1016/j.tws.2017.10.024.

[6] T. Green, N. Yazdani, F. Asce, L. Spainhour, and M. Asce, "Contribution of Intermediate Diaphragms in Enhancing Precast Bridge Girder Contribution of Intermediate Diaphragms in Enhancing Precast Bridge Girder Performance," vol. 3828, no. August 2004, pp. 3–8, 2017, doi: 10.1061/(ASCE)0887-3828(2004)18.

[7] A. Saber and W. Alaywan, "Full-Scale Test of Continuity Diaphragms in Skewed Concrete Bridge Girders," *J. Bridg. Eng.*, vol. 16, no. 1, pp. 21–28, 2011, doi: 10.1061/(asce)be.1943-5592.0000126.

[8] P. Qiao, M. Yang, D. I. Mclean, S. Antonio, W. Materials, and T. Building, "EFFECT OF INTERMEDIATE DIAPHRAGMS TO PRESTRESSED CONCRETE BRIDGE GIRDERS IN OVER-HEIGHT TRUCK IMPACTS," 1806.

[9] S. Maleki, P. Mohammadinia, and A. Dolati, "Numerical study of steel box girder bridge diaphragms," *Earthq. Struct.*, vol. 11, no. 4, pp. 681–699, 2016, doi: 10.12989/eas.2016.11.4.681.

[10] Z. (John) Ma, S. Chaudhury, J. L. Millam, and J. L. Hulsey, "Field Test and 3D FE Modeling of Decked Bulb-Tee Bridges," *J. Bridg. Eng.*, vol. 12, no. 3, pp. 306–314, 2007, doi: 10.1061/(asce)1084-0702(2007)12:3(306).

[11] B. F. Bender, "Prestressed Concrete Bridges," *ASCE J Constr Div*, vol. 103, no. 1, pp. 113–122, 1977, doi: 10.1680/bl.59979.137.

[12] Y. Fujino and D. Siringoringo, "Vibration mechanisms and controls of long-span bridges: A review," *Struct. Eng. Int. J. Int. Assoc. Bridg. Struct. Eng.*, vol. 23, no. 3, pp. 248–268, 2013, doi: 10.2749/101686613X13439149156886.

[13] V. N. Dinh, K. Du Kim, and D. T. Hai, *Riding Comfort Assessment of High-Speed Trains Based on Vibration Analysis*, vol. 54, no. January. Springer Singapore, 2020.

[14] Y. Fujino, D. M. Siringoringo, Y. Ikeda, T. Nagayama, and T. Mizutani, "Research and Implementations of Structural Monitoring for Bridges and Buildings in Japan," *Engineering*, vol. 5, no. 6, pp. 1093–1119, 2019, doi: 10.1016/j.eng.2019.09.006.

[15] Y. Fujino and D. M. Siringoringo, "Bridge monitoring in Japan: The needs and strategies," *Struct. Infrastruct. Eng.*, vol. 7, no. 7–8, pp. 597–611, 2011, doi: 10.1080/15732479.2010.498282.

[16] S. Chaiworawitkul, P. Omenzetter, and Y. Fujino, "Prediction of traffic-induced vibration using 3D bridge model and consideration of influence of bridge structural properties on response," *Proc. 2nd Int. Summer Symp. JSCE*, no. November 2014, 2000, doi: 10.13140/2.1.3406.4965.

[17] M. Tsubomoto, M. Kawatani, and K. Mori, "Traffic-induced vibration analysis of a steel girder bridge compared with a concrete bridge," *Steel Constr.*, vol. 8, no. 1, pp. 9–14, 2015, doi: 10.1002/stco.201510010.

[18] C. W. Kim, M. Kawatani, and W. S. Hwang, "Reduction of traffic-induced vibration of two-girder steel bridge seated on elastomeric bearings," *Eng. Struct.*, vol. 26, no. 14, pp. 2185–2195, 2004, doi: 10.1016/j.engstruct.2004.08.002.

[19] C. W. Kim, M. Kawatani, and K. B. Kim, "Three-dimensional dynamic analysis for bridge-vehicle interaction with roadway roughness," *Comput. Struct.*, vol. 83, no. 19–20, pp. 1627–1645, 2005, doi: 10.1016/j.compstruc.2004.12.004.

[20] M. I. Z. Ammar, E. Wahyuni, and D. Iranata, "Effects of Vibration Located on the Steel Truss Bridges under Moving Load," *IPTEK J. Proc. Ser.*, vol. 0, no. 1, p. 90, 2017, doi: 10.12962/j23546026.y2017i1.2198.

[21] B. Jeon, N. Kim, and S. Kim, "Estimation of the vibration serviceability deflection limit of a high-speed railway bridge considering the bridge-train interaction and travel speed Estimation of the Vibration Serviceability Deflection Limit of a High-speed Railway Bridge Considering the," no. May, 2015, doi: 10.1007/s12205-015-0565-z.

[22] P. Paultre, O. Chaallal, and J. Proulx, "Bridge dynamics and dynamic amplification factors - a review of analytical and experimental findings," *Can. J. Civ. Eng.*, vol. 19, no. 2, pp. 260–278, 1992, doi: 10.1139/l92-032.

[23] P. Museros, E. Moliner, and M. D. Martínez-Rodrigo, "Free vibrations of simply-supported beam bridges under moving loads: Maximum resonance, cancellation and resonant vertical acceleration," *J. Sound Vib.*, vol. 332, no. 2, pp. 326–345, 2013, doi: 10.1016/j.jsv.2012.08.008.

[24] B. M. Kato and S. Shimada, "This paper 3es the change of vibrational characteristics during the failure

process of prestressed-concrete-frame bridge by experiment and numerical analysis . The vibration test was carried out at each step of the static loading process until the bridge ," vol. 112, no. 7, pp. 1692–1703, 1986.

[25] D. Sekulić and V. Dedović, "The Effect of Stiffness and Damping of the Suspension System Elements on the Optimisation," *Int. J. Traffic Transp. Eng.*, vol. 2, no. 4, pp. 231–244, 2011.

[26] J. D. Yau, M. D. Martínez-Rodrigo, and A. Doménech, "An equivalent additional damping approach to assess vehicle-bridge interaction for train-induced vibration of short-span railway bridges," *Eng. Struct.*, vol. 188, no. March, pp. 469–479, 2019, doi: 10.1016/j.engstruct.2019.01.144.

[27] Z. Lu, Z. Wang, Y. Zhou, and X. Lu, "Nonlinear dissipative devices in structural vibration control: A review," *J. Sound Vib.*, vol. 423, pp. 18–49, 2018, doi: 10.1016/j.jsv.2018.02.052.

[28] C. Wang, S. Gao, L. Jin, and L. Chen, "Ambient Vibration Survey and Vibration Serviceability Evaluation on Footbridges," pp. 545–549, 2015, doi: 10.2991/cmfe-15.2015.127.

[29] M. Kawatani, Y. Kobayashi, and H. Kawaki, "Influence of elastomeric bearings on traffic-induced vibration of highway bridges," *Transp. Res. Rec.*, vol. 2, no. 1696, pp. 76–82, 2000, doi: 10.3141/1696-47.

[30] H. Moghimi and H. R. Ronagh, "Development of a numerical model for bridge-vehicle interaction and human response to traffic-induced vibration," *Eng. Struct.*, vol. 30, no. 12, pp. 3808–3819, 2008, doi: 10.1016/j.engstruct.2008.06.015.

[31] C. Z. Dong, S. Bas, and F. N. Catbas, "Investigation of vibration serviceability of a footbridge using computer vision-based methods," *Eng. Struct.*, vol. 224, no. August, p. 111224, 2020, doi: 10.1016/j.engstruct.2020.111224.

[32] B. Mullarney and P. Archbold, "Vibration Serviceability Considerations in Footbridge Design," no. January, 2016.

[33] L. Steel and G. Bridges, "INFLUENCE OF RAILING STIFFNESS ON SINGLE-SPAN TWO-," vol. 19, no. 73, pp. 33–40, 2020.

[34] X. Lu, C. W. Kim, and K. C. Chang, "Finite Element Analysis Framework for Dynamic Vehicle-Bridge Interaction System Based on ABAQUS," *Int. J. Struct. Stab. Dyn.*, vol. 20, no. 3, pp. 1–36, 2020, doi: 10.1142/S0219455420500340.

[35] V. Lukoševičius, R. Makaras, and A. Dargužis, "Assessment of tire features for modeling vehicle stability in case of vertical road excitation," *Appl. Sci.*, vol. 11, no. 14, 2021, doi: 10.3390/app11146608.

[36] W. K. Shi, C. Liu, Z. Y. Chen, W. He, and Q. H. Zu, "Efficient Method for Calculating the Composite Stiffness of Parabolic Leaf Springs with Variable Stiffness for Vehicle Rear Suspension," *Math. Probl. Eng.*, vol. 2016, 2016, doi: 10.1155/2016/5169018.

[37] L. Zhao, Y. Zhang, Y. Yu, C. Zhou, X. Li, and H. Li, "Truck handling stability simulation and comparison of taper-leaf and multi-leaf spring suspensions with the same vertical stiffness," *Appl. Sci.*, vol. 10, no. 4, 2020, doi: 10.3390/app10041293.

[38] J. Ke, C. Qian, Z. Wu, X. Hu, and Y. Yuan, "A theoretical model used for determining the stiffness of composite leaf springs with a main spring and an auxiliary spring," *J. Brazilian Soc. Mech. Sci. Eng.*,

vol. 42, no. 1, 2020, doi: 10.1007/s40430-019-2138-4.

[39] H. Iwabuki, S. Fukada, T. Osafune, M. Shimura, and E. Sasaki, "Contribution of large-vehicle vibration and bridge vibration to low-frequency noise generation characteristics," *Appl. Acoust.*, vol. 155, pp. 150–166, 2019, doi: 10.1016/j.apacoust.2019.05.011.

[40] D. Koulocheris and G. Papaioannou, "Dynamic analysis of the suspension system of a heavy vehicle through experimental and simulation procedure," *25th JUMV Int. Automot. Conf. "Science Mot. Veh.*, vol. 13, no. April, pp. 187–199, 2015.

[41] J. P. Pauwelussen, W. Dalhuijsen, and M. Merts, "Tyre Dynamics, Tyre as a Vehicle Component Part 1.: Tyre Handling Performance," *Virtual Educ. Rubber Technol. (VERT), FI-04-B-F-PP-160531*, pp. 29–47, 2007.

[42] T. Green, N. Yazdani, and L. Spainhour, "Contribution of Intermediate Diaphragms in Enhancing Precast Bridge Girder Performance," *J. Perform. Constr. Facil.*, vol. 18, no. 3, pp. 142–146, 2004, doi: 10.1061/(asce)0887-3828(2004)18:3(142).

[43] H. X. Le and E. S. Hwang, "Investigation of deflection and vibration criteria for road bridges," *KSCE J. Civ. Eng.*, 2017, doi: 10.1007/s12205-016-0532-3.

[44] K. R. K. Asapova and D. O. D. Inev, "HUMAN-INDUCED VIBRATIONS ON FOOTBRIDGES . CURRENT CODES OF PRACTICE – CASE STUDY," vol. 50, pp. 278–291, 2020.

[45] H. X. Le and E. S. Hwang, "Investigation of deflection and vibration criteria for road bridges," *KSCE J. Civ. Eng.*, vol. 21, no. 3, pp. 829–837, 2017, doi: 10.1007/s12205-016-0532-3.

[46] M. K. Ibrahim, A. Ab Rahman, and B. Hisham Ahmad, "Vehicle Induced Vibration on Real Bridge and Integral Abutment Bridge – A Short Review," *Appl. Mech. Mater.*, vol. 773–774, pp. 923–927, 2015, doi: 10.4028/www.scientific.net/amm.773-774.923.